

In-Context Learning Enhanced Credibility Transformer

Kishan Padayachy* Ronald Richman† Salvatore Scognamiglio‡

Mario V. Wüthrich§

September 11, 2025

Abstract

The starting point of our network architecture is the Credibility Transformer which extends the classical Transformer architecture by a credibility mechanism to improve model learning and predictive performance. This Credibility Transformer learns credibilized CLS tokens that serve as learned representations of the original input features. In this paper we present a new paradigm that augments this architecture by an in-context learning mechanism, i.e., we increase the information set by a context batch consisting of similar instances. This allows the model to enhance the CLS token representations of the instances by additional in-context information and fine-tuning. We empirically verify that this in-context learning enhances predictive accuracy by adapting to similar risk patterns. Moreover, this in-context learning also allows the model to generalize to new instances which, e.g., have feature levels in the categorical covariates that have not been present when the model was trained – for a relevant example, think of a new vehicle model which has just been developed by a car manufacturer.

Keywords. Transformer, Credibility Transformer, In-Context Learning, Attention Layer, Foundation Model, Insurance Pricing.

1 Introduction

A fundamental challenge in actuarial modeling lies in balancing predictive performance, explainability and reliable model estimation. This is especially true for risks for which one does not have a long observation history. Classical credibility theory, formalized by Bühlmann (1967) and Bühlmann and Straub (1970), provides an elegant framework for addressing this challenge through an optimal linear combination of instance individual and collective claims experience. In parallel, the machine learning community has developed sophisticated approaches for learning from limited data, culminating in the emergence of in-context learning (ICL) capabilities in large-scale Transformer models. The discovery that large-scale Transformers can adapt to new tasks through demonstration examples, revolutionized our understanding of few-shot learning Brown et al. (2020). That is, based on off-line training, a large-scale Transformer architecture

*insureAI, kishan@insureai.co

†insureAI and University of the Witwatersrand, ronaldrichman@gmail.com

‡Department of Management and Quantitative Sciences, University of Naples “Parthenope”, salvatore.scognamiglio@uniparthenope.it

§Department of Mathematics, ETH Zurich, mario.wuethrich@math.ethz.ch

can perform new tasks if sufficient context to these new tasks is provided, in particular, these tasks are done without retraining the Transformer architecture to the new situation. In some sense, this resembles the capability of being able to perform transfer learning. Recent theoretical work has established that this phenomenon can be understood as implicit gradient descent Akyürek et al. (2023), Bayesian inference Xie et al. (2022) and ICL on tabular data Hollmann et al. (2023) and Müller et al. (2024).

Recent work by Richman et al. (2025a) introduced the Credibility Transformer, demonstrating how classical credibility concepts can be embedded within modern Transformer architectures helping to improve the predictive performance of Transformers on tabular input data. Their approach leverages the CLS token mechanism of Devlin et al. (2019) to implement a learnable prior that is combined with feature-specific information through an attention-weighted averaging – similarly to linear Bühlmann (1967) credibility – achieving state-of-the-art performance on insurance datasets while maintaining explainability. A main benefit of this credibility mechanism that acts similar to drop-out during model training is the stabilization of the training algorithm leading to delayed early stopping points and better feature extraction.

However, existing approaches, including the Credibility Transformer, evaluate each risk in isolation during inference, neglecting potentially valuable information from similar observations within the portfolio. This limitation becomes particularly relevant in practical scenarios where insurers must price policies for risk profiles with limited historical experience while having access to recent claims data from similar risks, just think of expanding an existing insurance product to new geographical regions. The ability to leverage this contextual information dynamically, without retraining the model, may significantly enhance predictive accuracy and adapt to risk patterns of similar experience.

1.1 Literature review and background

1.1.1 Classical credibility theory

Credibility theory provides the theoretical foundation for combining individual experience with collective information in actuarial applications. The seminal work of Bühlmann (1967) and Bühlmann and Straub (1970) established the mathematical framework for an optimal linear prediction taking into account both sources of information. Generally, combining different sources of information involves intractable Bayesian posterior computations, and coping with this intractability, Bühlmann (1967) proposed a best-linear approximation by minimizing the mean squared error (MSE). This linear approximation takes the form

$$\hat{\mu} = \alpha Y + (1 - \alpha)\mu_0, \quad (1.1)$$

where Y reflects the individual experience, μ_0 is the collective information, and $\alpha \in [0, 1]$ is the *credibility weight* that weighs these two components. The credibility weight takes the form

$$\alpha = \frac{w}{w + \kappa},$$

where $w > 0$ is a case weight indicating the amount of information contained in the individual observation Y and $\kappa > 0$ is the *credibility coefficient* (hyper-parameter) that balances between individual and collective information. Basically, this credibility coefficient gives the trade-off between the different uncertainties involved at the individual and the collective level; see Bühlmann and Gisler (2005) for an extended discussion.

1.1.2 Transformer architectures for tabular data

The adaptation of the Transformer architecture of Vaswani et al. (2017) to tabular input data presents some challenges compared to their applications in large language models. Unlike sequential or grid-structured data, tabular features lack an inherent time-causal relationship for a canonical tensor encoding. This requires novel approaches to tokenization and positional encoding. The TabTransformer of Huang et al. (2020) pioneered the application of Transformers to tabular data by applying self-attention exclusively to categorical embeddings while processing continuous features through a separate pathway. This design choice reflects the observation that categorical variables often exhibit complex interactions that benefit from attention mechanisms, while continuous features may adequately be handled by simpler feed-forward neural network (FNN) layers.

The feature tokenizer (FT) Transformer of Gorishniy et al. (2021) extends this approach by tokenizing all features, both categorical and continuous ones, and processing them through a unified Transformer architecture. Their continuous feature tokenization uses a simple FNN embedding with an embedding space dimension being identical to the one chosen for the categorical entity embedding. This then naturally allows one to write the input feature in tensor form, which is the suitable structure for Transformer architectures. In an actuarial context, Brauer (2024) has empirically verified the excellent performance of these TF Transformer architectures on tabular input data.

Recent work on numerical feature encoding has explored various alternative approaches to handle continuous variables in Transformers. Noteworthy, piecewise linear encoding (PLE) of Gorishniy et al. (2022) provides a differentiable binning of continuous features that adapts to the data distribution. Periodic encoding using sinusoidal transformations Tancik et al. (2020) can capture cyclical patterns (maybe less relevant in general insurance pricing), while quantile-based encoding leverages distributional information for a robust feature representation.

1.1.3 In-context learning theory

ICL emerged as a surprising capability of large language models, where models can adapt to new tasks through demonstration examples provided in the input, without any parameter updates and model retraining; see Brown et al. (2020). This phenomenon has sparked intensive research into understanding the underlying mechanisms and theoretical foundations of ICL. Akyürek et al. (2023) demonstrated that linear self-attention layers can implement gradient descent on a MSE objective function when provided with appropriate in-context examples. Their analysis shows that Transformers can internally implement optimization algorithms, with attention weights encoding gradient information and value projections performing parameter updates. This finding suggests that ICL implements a form of implicit meta-learning within the forward pass. From a Bayesian perspective, Xie et al. (2022) and Müller et al. (2024) interpret ICL as implicit Bayesian inference, where the model maintains a posterior distribution over possible tasks and updates this posterior based on the context examples. Under this framework, the pre-trained distribution defines the prior, and attention mechanisms implement approximate posterior inference, providing a probabilistic foundation for understanding ICL behavior. This interpretation closes the loop to Bühlmann (1967), and it connects classical actuarial thinking with modern machine learning concepts.

Recent work has identified important factors that influence ICL performance. Min et al. (2022)

demonstrate that the format and distribution of demonstration examples matter more than their correctness, suggesting that ICL relies heavily on pattern matching and format recognition, while Wei et al. (2023) show that ICL capabilities emerge at scale, with larger models exhibiting qualitatively different learning behaviors than smaller ones.

Within the tabular learning context, where models are usually trained until performance on a validation loss is optimal, it would be surprising to find that ICL could lead to additional significant improvements in performance and – if this were to be the case – a new explanation for this improvement would be needed. Whereas Müller et al. (2024) have indeed shown that their TabICL model outperforms many other models, including models that only use supervised learning, as well as those using ICL, nonetheless, this could be explained by their extensive foundation model pre-training scheme using real and synthetic data. Classical supervised learning models are typically trained on a finite sample using early stopping of the gradient descent algorithm to prevent over-fitting. This early stopping may also prevent learning a more detailed, fine-grained structure, and foundation models being trained on a large body of (similar) data may be aware of such a detailed structure.

In this work, we would like to study the following questions: First, can ICL improve performance on a model that has been pre-trained using supervised learning? Second, if this is the case, what is the explanation for this improvement? Third, can ICL for tabular data be used to improve the performance of a much smaller pre-trained model focussing only on a single dataset?

1.1.4 Connections between credibility and meta-learning

The connection between actuarial credibility theory and modern meta-learning approaches has received limited attention despite their conceptual similarities. Both frameworks address the fundamental challenge of making predictions with limited task-specific data by leveraging broader experience. In credibility theory, this manifests as combining individual risk experience with portfolio-level information. In meta-learning, it involves leveraging experience across multiple tasks to enable rapid adaptation to new tasks. The mathematical structures underlying these approaches exhibit close parallels. The credibility formula in (1.1) can be viewed as a special case of prototype-based meta-learning, where the collective mean μ_0 serves as a prototype and the credibility factor α determines the adaptation strength. Similarly, the attention mechanisms in Transformers implement a form of non-parametric regression that generalizes credibility weighting to high-dimensional feature spaces. Recent work in neural processes Garnelo et al. (2018) provides a framework that unifies these perspectives. Neural processes implement a form of meta-learning that closely resembles Bayesian inference, with the context set defining a posterior distribution over functions. This framework naturally accommodates varying amounts of context information, analogous to how credibility factors adjust (based on available experience) through the case weights $w > 0$.

1.2 In-context learning enhanced Credibility Transformer

Our main contribution is the introduction of the In-Context Learning enhanced Credibility Transformer (ICL-Credibility Transformer), which combines the methods discussed in the previous subsections. First, the Credibility Transformer of Richman et al. (2025a) leverages the FT Transformer with a credibility mechanism that significantly enhances model training. A

crucial ingredient of the Credibility Transformer is the inclusion of the CLS token of Devlin et al. (2019), that is used to learn an encoding of the input information using the classical attention layer mechanism of Vaswani et al. (2017). But instead of simply encoding and extracting this CLS token, it is credibilized with a linear credibility mechanism that combines the feature individual CLS token encoding with a collective information token. This linear credibility combination has a very positive effect on gradient descent training, resulting in excellent predictive models. In fact, during gradient descent training, a randomized version of the credibility mechanism is applied that either selects the instance-specific CLS token or the collective information token. This randomized mechanism during model training can be interpreted as a drop-out mechanism, similar to Srivastava et al. (2014) and Wager et al. (2013), but instead of just dropping out and masking, at the same time a collective information representation is learned on the dropped out instances. This construction results in the credibilized CLS token which is a robustified encoding (representation) of the input data. The Credibility Transformer then processes these tokens through a decoder forming the predictions.

Inspired by the ICL architectures of Hollmann et al. (2023) and Müller et al. (2024) on tabular data, we modify the Credibility Transformer architecture to facilitate ICL. The crucial questions we were facing are:

- (1) At which stage should the predictive model on individual instances be augmented by context information?
- (2) How can this augmentation technically be done?
- (3) How can we ensure robustness of model learning?

The primary contributions of this paper are:

Architectural innovation. We introduce the ICL-Credibility Transformer, a novel architecture that extends the base Credibility Transformer with ICL capabilities. Our design features the following three ICL components that serve at augmenting the credibilized CLS tokens by context information including the response information of the context batch.

- (a) We design an *outcome token decorator* which augments the CLS tokens of the context batch by response information
- (b) We design a cross-batch attention mechanism that enables the instances of the target batch (to be predicted) to learn from the outcome augmented instances of the context batch. This context learning takes place in the space of the CLS tokens, i.e., in the same space as the original CLS tokens of the base Credibility Transformer live. This is enforced by reusing the frozen decoder from the base Credibility Transformer, as we discuss next.
- (c) We use the same projection layer as in the base Credibility Transformer to decode the outcome decorated CLS tokens. This is justified by the fact mentioned in item (b) saying that the ICL takes place in the space of the CLS tokens.

Theoretical framework. We establish formal connections between ICL mechanisms and classical credibility theory, proving that our ICL basically represents a credibility mechanism that regulates the impact of the context on the target instances to be predicted. We demonstrate

that the attention weights serve as adaptive, data-driven credibility factors that depend on both feature similarity and exposure levels, generalizing the fixed credibility weights of classical approaches.

Training methodology. We deploy a two-phase training strategy that first establishes strong feature representations through a standard supervised learning method of the base Credibility Transformer. This learned base Credibility Transformer already presents a strong predictive model. The second training phase fine-tunes the model using ICL. During this phase, we freeze the decoder layers (i.e., the output decoder) and train the ICL mechanism, as well as the base Credibility Transformer encoder. This constrained training approach enhances the robustness of the learning process, while allowing the weights of the base Credibility Transformer encoder which were initially optimized for supervised learning to be modified. Optionally, a third training step can be applied by jointly fine-tuning all network components, i.e., including the decoder layer; however, this requires careful regularization and a small learning rate to prevent performance degradation.

Empirical validation. We verify on the popular French Motor Third Party Liability (MTPL) dataset of Dutang et al. (2024) the outstanding performance of the ICL-Credibility Transformer. Our study quantifies the contribution of each architectural component, while explainability analyses reveal that the learned attention patterns align with actuarial intuition about risk similarity and credibility weighting. An interesting property of ICL is that we can explicitly illustrate and try to understand how individual instances in the context batch enhance the predictions; we provide empirical results explaining this case by case. A second interesting case study shows how the ICL-Credibility Transformer can be used to predict on data with new covariate levels, e.g., a new car brand that has not been available during model training. This generalization property (similar to transfer learning) especially draws on the context, to find the right level of integration into the existing model.

1.3 Manuscript organization

The next section introduces the ICL-Credibility Transformer. Starting from the base Credibility Transformer, we augment this base architecture by ICL that modifies the instance representations in the latent CLS token space by context batch information. This is achieved by a context token decorator and an ICL transformer. We also discuss the two phase learning procedure, which is common practice in contemporary machine learning tools. Section 3 mainly serves at giving model interpretations and making the connection to Bühlmann credibility. In Section 4, we verify the excellent performance of the ICL-Credibility Transformer on the popular French MTPL data of Dutang et al. (2024). In Section 5, we discuss a zero-shot analysis that shows how our method generalizes to new levels of features that have not been available for training, this reflects a sort of transfer learning using the context. Finally, Section 6 concludes.

2 In-context learning enhanced Credibility Transformer

This section defines the architecture of the ICL-Credibility Transformer. This architecture is crucially based on the groundbreaking work of Vaswani et al. (2017) on the attention layer mech-

anism and the Transformer architecture. Based on this seminal work, Richman et al. (2025a) introduced the Credibility Transformer which adapts the classical Transformer to tabular data and equips the architecture with a credibility mechanism that enhances learning and prediction. We will use the notation of Richman et al. (2025a).

2.1 ICL-Credibility Transformer architecture

The ICL-Credibility Transformer architecture consists of four main components:

- (1) a *Credibility Transformer encoder with a CLS token* that processes tabular features;
- (2) an *outcome token decorator* that encodes claims information;
- (3) an *ICL Transformer layer* that performs causal cross-batch attention; and
- (4) a *(frozen) decoder* that produces the final predictions.

We describe each component in detail in the following subsections.

2.1.1 Credibility Transformer encoder with CLS token

Our base Credibility Transformer (CT) follows the architecture introduced by Richman et al. (2025a), and we also use the notation of that reference. It takes an input \mathbf{x} and it outputs a prediction $\mu^{\text{CT}}(\mathbf{x})$. For this, it encodes the input \mathbf{x} into a learnable credibilized CLS token

$$\mathbf{x} \mapsto \mathbf{c}^{\text{cred}} = \mathbf{c}^{\text{cred}}(\mathbf{x}) \in \mathbb{R}^{2b},$$

for some encoding dimension $2b \in \mathbb{N}$; see Richman et al. (2025a, Formula (2.12)). This credibilized CLS token is a $2b$ -dimensional encoding of the feature \mathbf{x} (containing positional encodings). It is obtained by a Transformer architecture which is extended by the CLS token of Devlin et al. Devlin et al. (2019). During model fitting this CLS token is obtained by a credibility weighted average of individual instance information and global (prior) population information; see Richman et al. (2025a, Section 2.2).

The second part of the Credibility Transformer is the decoder $\mathbf{z}^{\text{decod}}$ which maps the credibilized CLS token to the prediction. Composing this encoder and decoder pair provides the base Credibility Transformer

$$\mathbf{x} \mapsto \mu^{\text{CT}}(\mathbf{x}) = (\mathbf{z}^{\text{decod}} \circ \mathbf{c}^{\text{cred}})(\mathbf{x}). \quad (2.1)$$

Training phase 1. This base Credibility Transformer (2.1) presents a supervised learning model. It is trained in a classical supervised learning manner by minimizing a loss function that compares the predictions $\mu^{\text{CT}}(\mathbf{x}_i)$ to the outcomes Y_i on an available learning sample $\mathcal{L} = (Y_i, \mathbf{x}_i, v_i)_{i=1}^n$; the variables $v_i > 0$ present case weights that may differ across the instances. This supervised learning step provides us with a fitted encoder $\hat{\mathbf{c}}^{\text{cred}}$, a fitted decoder $\hat{\mathbf{z}}^{\text{decod}}$ and a predictive model

$$\mathbf{x} \mapsto \hat{\mu}^{\text{CT}}(\mathbf{x}) = (\hat{\mathbf{z}}^{\text{decod}} \circ \hat{\mathbf{c}}^{\text{cred}})(\mathbf{x}). \quad (2.2)$$

This is precisely the predictive model considered in Richman et al. (2025a, Section 2.2), and in Table 2 of that reference it is verified on the popular French MTPL insurance dataset that this architecture provides an excellent predictive performance.

Broadly speaking, for all following steps, we keep the decoder layer (2.2) of the trained base Credibility Transformers fixed, i.e., we freeze the estimated weights of the fitted decoder \hat{z}^{decod} , but before we apply this frozen decoder \hat{z}^{decod} on the credibilized CLS tokens $\hat{c}^{\text{cred}} = \hat{c}^{\text{cred}}(\mathbf{x})$, we enrich these tokens by in-context information. We will start the ICL training from the weights of the encoder part of the model but we allow these to be optimized to produce a CLS token that is optimal for ICL.

2.1.2 Outcome token decorator

In the next step, we insert a module into the pre-calibrated base Credibility Transformer (2.2) that enables ICL. For this additional step, we assume that there are two kinds of data available. We have a *context batch* and we have a *target batch*. The target batch collects the instances whose responses need to be predicted, and this prediction is supported not only by the features of the target batch, but also by context data for which the responses are available.

We denote the context batch by $\mathcal{B}_{\text{context}} = (Y_j, \mathbf{x}_j, v_j)_{j \in \mathcal{I}_{\text{context}}}$ and the target batch is denoted by $\mathcal{B}_{\text{target}} = (Y_i, \mathbf{x}_i, v_i)_{i \in \mathcal{I}_{\text{target}}}$. These two sets are *disjoint* to avoid any leakage of information. The outcome token decorator is used to enrich the credibilized CLS tokens $\hat{c}^{\text{cred}}(\mathbf{x}_j)$ of the context set $j \in \mathcal{I}_{\text{context}}$ by outcome information Y_j (which we assume is available only on the context batch). This will then serve as the context to predict the instances in the target batch $\mathcal{B}_{\text{target}}$, where we assume that only the feature information \mathbf{x}_i and its encoded version $\hat{c}^{\text{cred}}(\mathbf{x}_i)$ is available to predict the response Y_i .

To simplify the notation, we merge the two index sets $\mathcal{I} = \mathcal{I}_{\text{target}} \cup \mathcal{I}_{\text{context}}$ assuming that these indices allow for a unique identification of all instances. We then introduce the mask for $i \in \mathcal{I}$

$$M_i = \begin{cases} 0 & \text{if } i \in \mathcal{I}_{\text{target}}, \\ 1 & \text{if } i \in \mathcal{I}_{\text{context}}. \end{cases}$$

This allows us to rewrite target and context batches in a unified batch

$$\mathcal{B} = (Y_i, \mathbf{x}_i, v_i, M_i)_{i \in \mathcal{I}}.$$

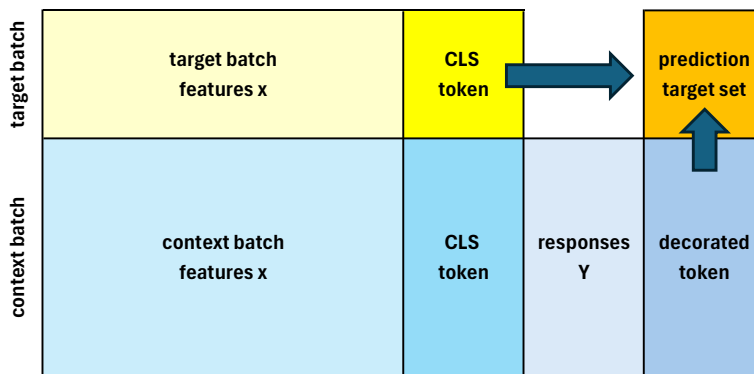


Figure 1: ICL-Credibility Transformer architecture processing the target batch $\mathcal{B}_{\text{target}}$ (yellow) and the context batch $\mathcal{B}_{\text{context}}$ (blue) to form the prediction on the target set (orange).

The following *outcome token decorator* only acts on the context batch, i.e., on the instances $i \in \mathcal{I}$ with $M_i = 1$. Let $\mathbf{z}^{\text{FNN1}} : \mathbb{R} \rightarrow \mathbb{R}^{2b}$ be a FNN network that embeds the responses into the same space as the credibilized tokens

$$Y \mapsto \mathbf{z}^{\text{FNN1}}(Y) \in \mathbb{R}^{2b}. \quad (2.3)$$

This outcome decorator will enrich the representations with claim information for instances in the context batch while maintaining causal consistency. The weights of this outcome token decorator \mathbf{z}^{FNN1} are learned in the second training phase, and this token decorator considers the unscaled responses Y not involving the case weights v , to avoid any leakage of information through the case weights. That is, in case of claims counts N , we simply select $Y = N$, which is achieved by setting $v \equiv 1$.

The *decorated tokens* are then defined by

$$\mathbf{c}^{\text{decor}}(\mathbf{x}_i) = \widehat{\mathbf{c}}^{\text{cred}}(\mathbf{x}_i) + \frac{v_i}{v_i + \kappa} M_i \mathbf{z}^{\text{FNN1}}(Y_i), \quad (2.4)$$

with

- credibilized tokens $\widehat{\mathbf{c}}^{\text{cred}}$, which, as above, have been produced using the encoder part of the original Credibility Transformer;
- we decorate all instances $i \in \mathcal{I}_{\text{context}}$ from the context batch $\mathcal{B}_{\text{context}}$ with encoded target information $\mathbf{z}^{\text{FNN1}}(Y_i)$;
- we integrate this target information using Bühlmann (1967) credibility, assigning a higher credibility for bigger case weights $v_i > 0$, and the credibility coefficient $\kappa > 0$ regulates the level of information considered; κ is a hyper-parameter that is either chosen by the modeler or learned during training.

Remark 2.1 The output token decorator (2.3) takes as inputs the unscaled responses Y . This will be suitable for our application which will consider low frequency claim counts, but it may need to be adapted in high frequency or high weight situations to weight-scaled versions. The credibility weights are adjusted such that we give lower credibility to observations with lower weights, emphasizing that these observations contain more uncertainty (irreducible risk from pure randomness). Moreover, for other applications, e.g., claim size modeling, one may also use the residuals $Y - \widehat{\mu}^{\text{CT}}(\mathbf{x})$ as inputs to the output token decorator. A pre-processing stage of the outcome token decorator should also consider transforming heavy-tailed or skewed responses, e.g., applying a log-transformation to heavy-tailed claim amounts, for a more efficient model training.

2.1.3 ICL Transformer

We are now equipped with the decorated tokens for all instances $i \in \mathcal{B}$ in the target and context batches, given by

$$\mathbf{c}^{\text{decor}}(\mathbf{x}_i) = \begin{cases} \widehat{\mathbf{c}}^{\text{cred}}(\mathbf{x}_i) & \text{if } i \in \mathcal{I}_{\text{target}}, \\ \widehat{\mathbf{c}}^{\text{cred}}(\mathbf{x}_i) + \frac{v_i}{v_i + \kappa} \mathbf{z}^{\text{FNN1}}(Y_i) & \text{if } i \in \mathcal{I}_{\text{context}}, \end{cases}$$

we also refer to Figure 1. The goal is to predict all the responses Y_i of the target set $i \in \mathcal{I}_{\text{target}}$ in one shot using the entire context batch $\mathcal{B}_{\text{context}}$. To ensure independence within the target set in the next step, we need to modify the previously introduced mask to

$$M_{i,j}^{\infty} = \begin{cases} -\infty & \text{if } i, j \in \mathcal{I}_{\text{target}} \text{ and } i \neq j, \\ 0 & \text{otherwise.} \end{cases}$$

This masks all pairs (i, j) in the target batch with $-\infty$ if their indices $i \neq j$ differ. This will imply that the instances in the target batch cannot interact. We define the mask tensor $\mathbf{M} = (M_{i,j}^{\infty})_{i,j \in \mathcal{I}}$, and we set $n = |\mathcal{I}|$ for the total batch size and $n_1 = |\mathcal{I}_{\text{target}}|$ for the target batch size.

Next, we define the causal ICL Transformer layer. We start by defining a causal attention layer; see Vaswani et al. (2017). Using three different time-distributed FNNs, we generate the query, key and value tensors, respectively,

$$\begin{aligned} \mathbf{Q} &= \left[\mathbf{z}_Q^{\text{FNN}} \left(\mathbf{c}^{\text{decor}}(\mathbf{x}_i) \right) \right]_{i \in \mathcal{I}}^{\top} \in \mathbb{R}^{n \times 2b}, \\ \mathbf{K} &= \left[\mathbf{z}_K^{\text{FNN}} \left(\mathbf{c}^{\text{decor}}(\mathbf{x}_i) \right) \right]_{i \in \mathcal{I}}^{\top} \in \mathbb{R}^{n \times 2b}, \\ \mathbf{V} &= \left[\mathbf{z}_V^{\text{FNN}} \left(\mathbf{c}^{\text{decor}}(\mathbf{x}_i) \right) \right]_{i \in \mathcal{I}}^{\top} \in \mathbb{R}^{n \times 2b}, \end{aligned}$$

for three time-distributed FNNs $\mathbf{z}_{\ell}^{\text{FNN}}$ having an identical architecture but different network weights for $\ell \in \{Q, K, V\}$. These three tensors are used to define the *causal self-attention head*

$$\mathbf{H} = \mathbf{H}(\mathbf{Q}, \mathbf{K}, \mathbf{V}, \mathbf{M}) = \mathbf{A}\mathbf{V} \in \mathbb{R}^{n \times 2b}, \quad (2.5)$$

with *causal attention layer*

$$\mathbf{A} = \mathbf{A}(\mathbf{Q}, \mathbf{K}, \mathbf{M}) = \text{softmax} \left(\mathbf{Q}\mathbf{K}^{\top} / \sqrt{2b} + \mathbf{M} \right) \in \mathbb{R}^{n \times n},$$

where the softmax operator is applied row-wise. This allows us to define the *ICL Transformer layer* as follows. First, we define the decorated token tensor

$$\mathbf{C}^{\text{decor}} = \left[\mathbf{c}^{\text{decor}}(\mathbf{x}_i) \right]_{i \in \mathcal{I}}^{\top} \in \mathbb{R}^{n \times 2b}.$$

The ICL Transformer layer includes two skip connections, another time-distributed FNN $\mathbf{z}^{\text{t-FNN2}}$, and dropout layers and layer-normalization layers. The first regularized skip connection is given by

$$\mathbf{C}^{\text{mid}} = \text{LayerNorm} \left(\mathbf{C}^{\text{decor}} + \text{Dropout}(\mathbf{H}) \right).$$

This then allows one to compute the ICL Transformer output

$$\mathbf{C}^{\text{ICL-trans}} = \text{LayerNorm} \left(\mathbf{C}^{\text{mid}} + \text{Dropout} \left(\mathbf{z}^{\text{t-FNN2}} \left(\mathbf{C}^{\text{mid}} \right) \right) \right) \in \mathbb{R}^{n \times 2b}. \quad (2.6)$$

2.1.4 Frozen decoder

The last step is to decode the ICL Transformer tensor $\mathbf{C}^{\text{ICL-trans}}$ to form the predictions on the target batch, i.e., for the responses Y_i , $i \in \mathcal{I}_{\text{target}}$. For this we use the frozen decoder $\hat{\mathbf{z}}^{\text{decod}}$

from the first training phase. This architectural constraint ensures that all ICL computations operate within the original representation space learned during the first learning phase, which provides some theoretical elegance and practical benefits that maintain the interpretability of the original space in which the CLS tokens live.

Let us denote the row vectors of the tensor $\mathbf{C}^{\text{ICL-trans}}$ as follows

$$\mathbf{C}^{\text{ICL-trans}} = \left[\mathbf{c}_1^{\text{ICL-trans}}, \dots, \mathbf{c}_{n_1}^{\text{ICL-trans}}, \mathbf{c}_{n_1+1}^{\text{ICL-trans}}, \dots, \mathbf{c}_n^{\text{ICL-trans}} \right]^\top \in \mathbb{R}^{n \times 2b},$$

where the first $n_1 = |\mathcal{I}_{\text{target}}|$ rows belong to the target batch $\mathcal{B}_{\text{target}}$ for which we would like to predict the responses Y_i , $i \in \mathcal{I}_{\text{target}}$, and the remaining rows correspond to the context batch. Applying the frozen decoder provides us in analogy to (2.2) with

$$\hat{\mu}^{\text{ICL-CT}}(\mathbf{x}_i; \mathcal{B}_{\text{context}}) = \hat{\mathbf{z}}^{\text{decod}}\left(\mathbf{c}_i^{\text{ICL-trans}}\right), \quad \text{for } i \in \mathcal{I}_{\text{target}}. \quad (2.7)$$

We give some remarks.

- *Calibration preservation:* The output scale and the calibration learned during the first training phase are preserved by keeping the weights of the decoder fixed during the second training phase (being discussed below).
- *Implicit regularization:* By constraining the ICL mechanism to operate within the learned representation space, we prevent it from arbitrarily transforming representations in ways that might over-fit to the ICL training objective. This acts as a strong regularization mechanism.
- *Transfer learning efficiency:* The frozen decoder ensures that the ICL mechanism leverages the full predictive power of the pre-trained model of the first training phase rather than relearning the entire prediction function. The ICL components only need to learn the context-aware adjustments within the existing representation space.
- *Gradient flow simplification:* During the ICL fine-tuning (second training phase), the gradients flow through the ICL Transformer and the outcome token decorator, but they stop at the frozen decoder, simplifying the optimization landscape and reducing the risk of forgetting of the pretrained representations.
- *Information bottleneck:* From a more information-theoretic perspective, the frozen decoder enforces an information bottleneck that prevents the ICL mechanism from encoding arbitrary information that was not present in the original representation space. This aligns with the principle of minimal sufficient statistics, ensuring that the ICL mechanism focuses on extracting and utilizing the most relevant contextual information for improving predictions. On the other hand, this also requires that the learned credibilized CLS tokens $\hat{\mathbf{c}}^{\text{cred}}$ are sufficiently rich, otherwise the ICL fine-tuning will not have any positive effect on improving the Credibility Transformer predictions.

Training phase 2. This second training phase is essentially an ICL fine-tuning. This ICL fine-tuning acts on

1. the encoder of the original Credibility Transformer;

2. the outcome token decorator (2.4), this involves the response embedding \mathbf{z}^{FNN1} and the credibility coefficient κ ;
3. the ICL Transformer, this involves the Transformer architecture (2.6) including the attention mechanism and the skip connections architecture.

The outputs of the ICL-Credibility Transformer architecture are the predictions (2.7) on the target batch. This motivates to consider the loss function for the second training phase

$$\mathcal{L}_{\text{ICL}}(\mathcal{B}_{\text{target}}; \mathcal{B}_{\text{context}}) = \frac{1}{|\mathcal{I}_{\text{target}}|} \sum_{i \in \mathcal{I}_{\text{target}}} v_i L(Y_i, \hat{\mu}^{\text{ICL-CT}}(\mathbf{x}_i; \mathcal{B}_{\text{context}})), \quad (2.8)$$

for a suitable loss function L (comparing responses Y and predictions $\hat{\mu}$) and case weights $v > 0$. In practice, we will have many target-context pairs, and this second training phase performs gradient descent fine-tuning on all these pairs, averaging the losses (2.8) of the the available target-context pairs.

2.2 Learning procedure

The fitting procedure presented above has two different learning phases. The first one is used to learn the credibilized CLS token encoder $\hat{\mathbf{c}}^{\text{cred}}$ and the decoder $\hat{\mathbf{z}}^{\text{decod}}$, respectively, and the second phase is used to learn the context augmentation involving the context token decorator and the ICL Transformer, as well as fine-tuning the CLS token decorator. This two step approach is employed for computational reasons and for robustifying the training procedure. There is one critical point in this two stage procedure though, namely, one needs to ensure that the learned credibilized CLS tokens $\hat{\mathbf{c}}^{\text{cred}}(\mathbf{x}_i)$, $i \in \mathcal{I}$, are sufficiently rich and carry sufficient information of the inputs \mathbf{x}_i ; an encoding can be thought of a data compression. The critical point is that the training of the encoder $\hat{\mathbf{c}}$ and the decoder $\hat{\mathbf{z}}^{\text{decod}}$ only focuses on optimal predictive performance, without accounting for the space of encoded features $(\hat{\mathbf{c}}^{\text{cred}}(\mathbf{x}))_{i \in \mathcal{I}}$ being still sufficiently rich to be able to benefit from ICL in the second step. Basically, there are two ways of ensuring this. First, certainly the embedding dimension $2b$ of the CLS tokens should be sufficiently large, otherwise we are facing the bottleneck already in the very beginning. Second, one can employ a third training phase, allowing for fine-tuning of all involved weights by jointly training the entire architecture starting from the pre-trained weights of the first two phases. To ensure stability of the learned representation space, this third (fine-tuning) step should be constrained by a strong regularization or it should only consider very few gradient descent steps with moderate step sizes.

Clearly, to benefit from context data, the target batch and the context batch have to be associated. This association can reflect target-context pairs that consider the same products, the same local regions or the same circumstances in which these instances operate, without having these (soft) factors encoded in the features. Such examples are the most obvious ones in which the ICL-Credibility Transformer can successfully operate. A less obvious though similar set-up is the problem of having a high-cardinality categorical feature, e.g., vehicle models within a motor insurance portfolio. Categorical encoding (one-hot encoding, dummy coding or entity embedding) will then involve a vast number of parameters which cannot be estimated reliably (with credibility). Instead of trying to estimate a multitude of parameters, we rather could use similar instances as the context batch. Either there is a natural association or one can try to construct

a neighborhood of similar instances using an unsupervised learning method; see Wüthrich et al. (2025, Chapter 10).

Alternatively, one could also select a context batch that is not directly retrieval-related, but one rather uses this second training phase as a fine-tuning phase. That is, the base Credibility Transformer may not have learned the optimal CLS tokens because the early stopping may not only prevent from over-fitting, but it may also prevent from sufficient fine-tuning. The second training phase with the context-augmented information can then be seen as the fine-tuning phase that tries to find the structure that was not found by the base Credibility Transformer training with early stopping. This view can also be interpreted as a boosting step.

3 Bühlmann credibility and interpretations

We establish a theoretical connection between the ICL mechanism and linear Bühlmann (1967) credibility. In the ICL setting, we partition our data into context and target batches, $\mathcal{B} = \mathcal{B}_{\text{context}} \cup \mathcal{B}_{\text{target}}$. The ICL objective is to enhance predictions on the target batch augmenting the available information by the context batch. There are multiple credibility mechanisms involved in this architecture. Besides the base Credibility Transformer, there is the obvious one giving the decorated tokens (2.4). The weights $v_i/(v_i + \kappa)$ in these decorated tokens precisely reflect linear Bühlmann (1967) credibility that assigns a higher credibility weight for bigger case weights v_i . E.g., in claims counts modeling this is used to balance the different exposure lengths between the instances for experience rating. The following proposition unveils a more hidden credibility.

Proposition 3.1 *The attention mechanism in the causal attention head $\mathbf{H} = [\mathbf{h}_1, \dots, \mathbf{h}_n]^\top \in \mathbb{R}^{n \times 2^b}$, given in (2.5), has the following credibility structure for every instance $i \in \mathcal{I}_{\text{target}}$ of the target batch*

$$\mathbf{h}_i = a_{i,i} \mathbf{z}_V^{\text{FNN}} \left(\widehat{\mathbf{c}}^{\text{cred}}(\mathbf{x}_i) \right) + \sum_{j \in \mathcal{I}_{\text{context}}} a_{i,j} \mathbf{z}_V^{\text{FNN}} \left(\widehat{\mathbf{c}}^{\text{cred}}(\mathbf{x}_j) + \frac{v_j}{v_j + \kappa} \mathbf{z}^{\text{FNN1}}(Y_j) \right), \quad (3.1)$$

with attention weights $a_{i,j} \geq 0$ satisfying $a_{i,i} + \sum_{j \in \mathcal{I}_{\text{context}}} a_{i,j} = 1$, the specific structure is given in (3.3), below.

A consequence of this result is that the attention head performs a credibility weighting between instance i specific information and the augmented context information. Note that this credibility step is the only step where targets and the context interact. In terms of explainability, we can extract the learned attention weights $(a_{i,j})_{j \in \mathcal{I}_{\text{context}} \cup \{i\}}$ to indicate from which context instance we can learn the most for a specific instance i of the target batch.

This explanation (3.1) looks rather convincing, however, it hides an essential feature that makes this consideration different from linear Bühlmann (1967) credibility. Namely, the responses $(Y_j)_{j \in \mathcal{I}_{\text{context}}}$ also enter the attention weights $(a_{i,j})_{j \in \mathcal{I}_{\text{context}} \cup \{i\}}$; not being expressed in this notation. That is, in fact, we have a non-linear structure (3.1) in the responses $(Y_j)_{j \in \mathcal{I}_{\text{context}}}$ and a linear Bühlmann (1967) credibility interpretation only reflects a first order statement. This point could be modified to a proper linear credibility formula by considering the changed query

and key tensors

$$\begin{aligned}\tilde{\mathbf{Q}} &= \left[\mathbf{z}_Q^{\text{FNN}} \left(\mathbf{c}^{\text{cred}}(\mathbf{x}_i) \right) \right]_{i \in \mathcal{I}}^{\top} \in \mathbb{R}^{n \times 2b}, \\ \tilde{\mathbf{K}} &= \left[\mathbf{z}_K^{\text{FNN}} \left(\mathbf{c}^{\text{cred}}(\mathbf{x}_i) \right) \right]_{i \in \mathcal{I}}^{\top} \in \mathbb{R}^{n \times 2b}, \\ \mathbf{V} &= \left[\mathbf{z}_V^{\text{FNN}} \left(\mathbf{c}^{\text{decor}}(\mathbf{x}_i) \right) \right]_{i \in \mathcal{I}}^{\top} \in \mathbb{R}^{n \times 2b},\end{aligned}\tag{3.2}$$

i.e., changing the queries and keys to purely feature driven (excluding the responses), would give a proper linear credibility formula in the observations Y_j in (3.1). This option can easily be used if we have a single ICL Transformer layer, but cannot easily be adapted to deep ICL Transformers.

Proof. The proof is an easy consequence of the attention mechanism in the attention head (2.5). Focusing on the i -th row of the causal attention layer \mathbf{A} , we have through the softmax operator

$$a_{i,j} = \frac{\exp \left(\mathbf{q}_i^{\top} \mathbf{k}_j / \sqrt{2b} + M_{i,j}^{\infty} \right)}{\sum_{k=1}^n \exp \left(\mathbf{q}_i^{\top} \mathbf{k}_k / \sqrt{2b} + M_{i,k}^{\infty} \right)} > 0, \quad \text{for } j \in \mathcal{I},$$

with query tensor $\mathbf{Q} = [\mathbf{q}_1, \dots, \mathbf{q}_n]^{\top}$ and key tensor $\mathbf{K} = [\mathbf{k}_1, \dots, \mathbf{k}_n]^{\top}$. The softmax operator normalizes this to 1, thus, $(a_{i,j})_{j=1}^n$ reflect normalized weights. If we select an instance from the target set $i \in \mathcal{I}$, we receive through the masking operator \mathbf{M}

$$a_{i,j} = \frac{\exp \left(\mathbf{q}_i^{\top} \mathbf{k}_j / \sqrt{2b} \right)}{\exp \left(\mathbf{q}_i^{\top} \mathbf{k}_i / \sqrt{2b} \right) + \sum_{k \in \mathcal{I}_{\text{context}}} \exp \left(\mathbf{q}_i^{\top} \mathbf{k}_k / \sqrt{2b} \right)} \in (0, 1), \quad \text{for } j \in \mathcal{I}_{\text{context}} \cup \{i\},\tag{3.3}$$

and $a_{i,j} = 0$ if $j \in \mathcal{I}_{\text{target}} \setminus \{i\}$. The latter ensures that there is no interaction within the target batch, and the remainder gives the classical credibility structure on $\mathcal{I}_{\text{context}} \cup \{i\}$. Inserting this into the attention head (2.5) gives us for the target instances $i \in \mathcal{I}_{\text{target}}$

$$\begin{aligned}\mathbf{h}_i &= \sum_{j \in \mathcal{I}} a_{i,j} \mathbf{v}_j = a_{i,i} \mathbf{v}_i + \sum_{j \in \mathcal{I}_{\text{context}}} a_{i,j} \mathbf{v}_j, \\ &= a_{i,i} \mathbf{z}_V^{\text{FNN}} \left(\hat{\mathbf{c}}^{\text{cred}}(\mathbf{x}_i) \right) + \sum_{j \in \mathcal{I}_{\text{context}}} a_{i,j} \mathbf{z}_V^{\text{FNN}} \left(\hat{\mathbf{c}}^{\text{cred}}(\mathbf{x}_j) + \frac{v_j}{v_j + \kappa} \mathbf{z}^{\text{FNN1}}(Y_j) \right),\end{aligned}$$

for value tensor $\mathbf{V} = [\mathbf{v}_1, \dots, \mathbf{v}_n]^{\top}$. This completes the proof. \square

4 Numerical example

We evaluate our approach on the well-known French MTPL dataset of Dutang et al. (2024), which has been widely studies in the recent actuarial literature. The dataset contains policy-level information with claim frequencies, allowing us to assess the proposed ICL-Credibility Transformer model's ability to predict insurance claim rates. The characteristics of the dataset are summarized in Table 1.¹

The dataset exhibits typical characteristics of insurance portfolios: highly imbalanced with most policies having zero claims, heterogeneous exposure periods, and a mix of categorical and continuous risk factors.

¹We use the data-cleaned version that can be downloaded from <https://aitools4actuaries.com/>.

Table 1: Dataset characteristics

Characteristic	Training set	Test set
Number of policies	610,206	67,801
Total exposure (years)	322,857	35,943
Number of claims	23,738	2,645
Average frequency	7.36%	7.35%
Feature description		
Categorical (4): Area, VehGas, VehBrand, Region		
Continuous (5): VehPower, VehAge, DrivAge, BonusMalus, Density		
Target: ClaimNb (claim count)		
Exposure: Exposure (in years)		

We use the Poisson deviance loss as our primary loss metric, consistent with actuarial practice and presenting a strictly consistent scoring function, see Gneiting and Raftery (2007),

$$L_{\text{Poisson}} = \frac{2}{n} \sum_{i=1}^n \left[\hat{\mu}_i - Y_i - Y_i \log \left(\frac{\hat{\mu}_i}{Y_i} \right) \right],$$

with $\hat{\mu}_i = \hat{\mu}(\mathbf{x}_i)$ being the predictor for the claim Y_i .

We report on two main versions of the ICL-Credibility Transformer. The first one is exactly the ICL-Credibility Transformer as described in the previous section with the non-linear credibility mechanism in the attention head, see (3.1). The second one is the simpler linearized ICL-Credibility Transformer, where we restrict the queries and keys to be purely feature driven (excluding the responses), see (3.2). For the former model, we utilize two ICL Transformer layers and for the latter model, we utilize one ICL Transformer layer, so as to preserve the linear credibility structure, as discussed above. The training will have three phases. In the first phase, for both of the models, we perform a single training run on the base Credibility Transformer model. For this, we select the AdamW optimizer (learning rate 10^{-3} , weight decay 10^{-2} , $\beta_2 = 0.95$), batch size 1024, Poisson deviance loss, and a 15% validation split with early stopping (patience 20). Then, we freeze the CT model’s decoder and insert the outcome token decorator and the ICL Transformer layers between the CLS token and the output of the Credibility Transformer model. In this second training phase, we train the ICL Transformer, base Credibility Transformers encoder and the initial embedding weights for 50 epochs with the AdamW optimizer (learning rate $3 \cdot 10^{-4}$, weight decay 10^{-2} , $\beta_2 = 0.95$) while maintaining causal masking so that target examples do not interact. In other words, we keep only the decoder frozen in this training step, and allow all other weights, including those of the CT, to be modified. Batches are constructed as a concatenation of a context set and a held-out chunk of examples, and we apply the loss only on the held-out chunk via sample weights. The final third phase performs a fine-tuning step of the entire architecture for 20 epochs, i.e., including all of the components of the ICL-Credibility Transformer (the base Credibility Transformer, the context token decorator, the ICL transformer and the decoder) with a small AdamW learning rate $3 \cdot 10^{-5}$ and early stopping (patience 10).

The instances within the context batches are selected so as to be similar to the instances with the target batches. This is done by performing an approximate neighborhood search of the target instances within the context batch. For each step, we assemble batches as $[\mathcal{B}_{\text{context}} \parallel \mathcal{B}_{\text{target}}]$ with

context size $c = \min(1000, |\mathcal{D}_{\text{train}}|)$ and target chunk size $m = 200$, i.e., we use a ratio of 5 context rows for each target row. At inference, we partition the test set into chunks of size $m = 200$. For each chunk, we compute base-encoder embeddings for the m test rows and retrieve their top- $(K = 64)$ nearest neighbors from the training set (cosine via inner product on ℓ_2 -normalized vectors, see next paragraph). We take the union of all retrieved neighbors across the chunk, deduplicate, rank globally by best similarity to any test row, and retain the top $c = 1000$ as the context set. We then form a batch $[\mathcal{B}_{\text{context}} \parallel \mathcal{B}_{\text{target}}]$, supply observed responses only for $\mathcal{B}_{\text{context}}$ (zeros for $\mathcal{B}_{\text{target}}$), and apply a causal mask that prevents target-target interactions while allowing target-context attention. A single forward pass yields predictions for the target block; we keep the last m outputs and iterate over all chunks to cover the full test set.

To form $\mathcal{B}_{\text{context}}$ for each target chunk, we retrieve neighbors from the base Credibility Transformer model’s CLS token embedding space; we interpret similarity in the CLS token as similarity in risk behavior. By default, we use cosine similarity implemented as inner product on ℓ_2 -normalized embeddings. We query $K = 64$ nearest neighbors per target example and then build a unique candidate pool by taking the union across the target chunk and ranking candidates by similarity. After ranking by similarity, we take the top $c = 1000$ candidates². We employ the FAISS package (Johnson et al., 2019) for high-throughput nearest neighbor search. For a summary, see Table 2.

Table 2: Key implementation hyper-parameters (ICL)

Component	Setting
Base CT pretraining	AdamW (LR 10^{-3} , WD 10^{-2} , $\beta_2 = 0.95$), 100 epochs, batch 1024
ICL fine-tuning	AdamW (LR $3 \cdot 10^{-4}$, WD 10^{-2} , $\beta_2 = 0.95$), 50 epochs
Joint fine-tuning	AdamW (LR $3 \cdot 10^{-5}$), 20 epochs
Objective	Poisson deviance loss
Validation	Early stopping: base CT pre-train 20, ICL 20, joint 10 (patience)
Batching	Context $c = 1000$, target chunk $m = 200$; loss on target rows only
Retrieval metric	Cosine similarity
Neighbors	$K = 64$ per target; union, optional per-target quota, cap at c
Pre-computation	Train→train neighbors (default on); optional val/test→train; on-disk cache

We compare the ICL-Credibility Transformer against several baselines taken from Wüthrich and Merz (2023), Brauer (2024), Richman et al. (2025a) and Richman et al. (2025b). Table 3 presents the out-of-sample performance comparison across all models.

Generally, because stochastic gradient descent fitting involves several items of randomness, e.g., through the random initializations of the algorithms, we perform 5 fitting runs for all architectures, and the shown results are averages over these 5 fitting runs; in brackets we provide the observed standard deviations. The single run of the base Credibility Transformer produces a result of 23.743 (out-of-sample), which is roughly within 1 standard deviation of the results obtained in the original Credibility Transformer model 23.788 ± 0.040 . Adding the context

²In more detail, for each test chunk of size m , we retrieve the top- K nearest training neighbors per test row in the base embedding space (cosine via inner product on ℓ_2 -normalized vectors). Let $\mathcal{N}(x_r)$ denote the K neighbors of test point x_r and define the candidate pool $\mathcal{C} = \bigcup_{r=1}^m \mathcal{N}(x_r)$. We assign each candidate $j \in \mathcal{C}$ a single score given by its best match over the chunk, namely $s_j = \max_r \text{sim}(x_r, j)$ for cosine similarity. We then sort the candidates by s_j in descending order for the cosine similarity, break ties deterministically, and select the first $c = 1000$ unique items as the context set.

Model	# Param.	In-sample Poisson loss	Out-of-sample Poisson loss
Null model (intercept-only)	1	25.213	25.445
Poisson GLM3	50	24.084	24.102
Poisson GAM	(66.7)	23.920	23.956
Plain-vanilla FNN	792	23.728 (± 0.026)	23.819 (± 0.017)
Ensemble plain-vanilla FNN	792	23.691	23.783
CAFFT	27,133	23.715 (± 0.047)	23.807 (± 0.017)
Ensemble CAFFT	27,133	23.630	23.726
Credibility Transformer	1,746	23.641 (± 0.053)	23.788 (± 0.040)
Ensemble Credibility Transformer	1,746	23.562	23.711
Tree-like PIN	4,147	23.593 (± 0.046)	23.740 (± 0.025)
Ensemble Tree-like PIN	4,147	23.522	23.667
Single run base Credibility Transformer (phase 1)	15,614	23.653	23.743
ICL Transformer - 2 Layers (phase 2)	46,439	23.631 (± 0.048)	23.725 (± 0.022)
Ensemble ICL Transformer - 2 Layers (phase 2)	46,439	23.584	23.679
ICL Transformer Fine-tuning (phase 3)	46,439	23.561 (± 0.024)	23.710 (± 0.009)
Ensemble ICL Transformer Fine-tuning (phase 3)	46,439	23.521	23.676
ICL Transformer Linearized (phase 2)	33,199	23.634 (± 0.046)	23.766 (± 0.034)
Ensemble ICL Transformer Linearized (phase 2)	33,199	23.570	23.699
ICL Transformer Linearized Fine-tuning (phase 3)	33,199	23.563 (± 0.043)	23.723 (± 0.041)
Ensemble ICL Transformer Linearized Fine-tuning (phase 3)	33,199	23.514	23.678

Table 3: Number of parameters, in-sample and out-of-sample Poisson deviance losses (units are in 10^{-2}). Benchmark models for Null model through Poisson GAM are taken from Wüthrich and Merz (2023, Table 7.9); plain-vanilla FNN and ensemble results are from Wüthrich and Merz (2023, Table 7.9); CAFFT results are from Brauer (2024, Tables 2 and 4); Credibility Transformer results are from Richman et al. (2025a, Table 2); Tree-like PIN results are from Richman et al. (2025b, Table 2).

token decorator and the ICL Transformer to the base Credibility Transformer model produces small out-of-sample improvements for the version with two layers 23.725; however, the linearized version yields 23.766 (out-of-sample), demonstrating a slight worsening in performance. Fine-tuning all parameters of the ICL-Credibility Transformer produces further small improvements, with the fine-tuned non-linear ICL-Credibility Transformer version achieving the best test performance 23.710 compared to 23.723 for the linearized version. This latter point means that the linearized version benefits from ICL once full fine-tuning is performed. The scores discussed thus far for the linearized and two-layer models are the average scores of 5 independent fitting runs (as mentioned at the beginning of this paragraph).

The best scores are achieved after ensembling (averaging) the predictions of the 5 independent fitting runs together. The scores improve after ensembling the 5 models, with the linearized model achieving a score of 23.699 before fine-tuning and 23.678 after fine-tuning. The best out-of-sample ICL results are achieved by the two-layer model, with 23.679 pre-fine-tuning and 23.676 post-fine-tuning. Notably, the simpler linearized model performs almost as well as the larger non-linear model after fine-tuning.

We observe that the ICL models have quite dramatically improved upon the results of the

original Credibility Transformer. Thus, we are now able to answer the remaining two questions with which we opened this paper. The ICL-Credibility Transformer improves performance on a basic Credibility Transformer model, which in itself achieves a good out-of-sample performance, both for the ICL-Credibility Transformer version with two layers and for the linearized version. Thus, the first opening question is answered in the affirmative. Moreover, we have shown that the ICL approach improves the performance of a much smaller model focusing only on a single dataset, with the 2 layer ICL-Credibility Transformer fine-tuned version achieving the best test performance. Thus, the third opening question is also answered in the affirmative. Remarkably, this means that the credibility mechanism implemented by the ICL Transformer approach taken in this paper can improve on supervised learning for actuarial applications!

We now analyze how the steps taken to build the ICL-Credibility Transformer affect the CLS tokens and the predictions. For simplicity, we select a single run of the ICL-Credibility Transformer training and perform a principal component analysis (PCA) of the CLS tokens within the test set of the base Credibility Transformer model; then, we transform the following vectors from the models using this same fitted PCA analysis: the CLS token of the original CT before modifying this model, the decorated CLS tokens before the ICL mechanism, the decorated CLS tokens after ICL augmentation, the CLS tokens after fine-tuning the ICL-Credibility Transformer end to end, the decorated CLS tokens after fine-tuning the ICL-Credibility Transformer and, finally, the decorated CLS tokens after fine-tuning the ICL-Credibility Transformer and performing ICL. Because we use the same PCA analysis for all of the models, we can directly compare the projections of the CLS tokens and the predictions. Figure 2 shows the results of this analysis for ten points selected as the deciles of the original CT frequency predictions in the test set.

From the plots, we can see that the ten points undergo quite a progression from the original CLS tokens to the decorated CLS tokens after ICL, to the CLS tokens after performing ICL; fine-tuning the model end-to-end seems slightly to shrink the space inhabited by the tokens and also to shrink the most extreme predictions somewhat. To better understand this progression, we show in Figure 3 the total progression of the ten points in the PCA space, labeling the original CT predictions made for that point, the predictions after allowing the weights of the CT model to be modified and the final predictions after ICL in the fine-tuned model.

To provide a more qualitative analysis of the progression of the ten points in the PCA space, we search for the five nearest neighbors of each of the tokens of the ten points in the various different token spaces we have described above. We then compare each point with each of its neighbors to see how the predictions change. For the explicit numerical results of the following summarized description, we refer to the appendix.

Outcome decoration consistently tightens neighborhoods, with the closest-match distance typically reduced by 10-40%; for example, point 1 shrinks from ≈ 0.35 (pre-base) to ≈ 0.30 (pre-decorated), point 3 from ≈ 0.018 to ≈ 0.011 , and point 9 from ≈ 0.32 to ≈ 0.21 . The subsequent “final” stages generally broaden the local set slightly, admitting a few nearby but more heterogeneous neighbors (adjacent Regions, alternative brands, or the other fuel type) while preserving the some of the more important covariates (Area, Region, Driver Age, and Bonus-Malus). Across the points we analyze, Region and fuel coherence dominate: decoration strengthens these alignments (e.g., R11 regular drivers for point 9; R24 diesels for points 3, 4, and 10). Brand resolution also improves: decoration often pulls exact brand matches into the top set (e.g., B14 for point 2;

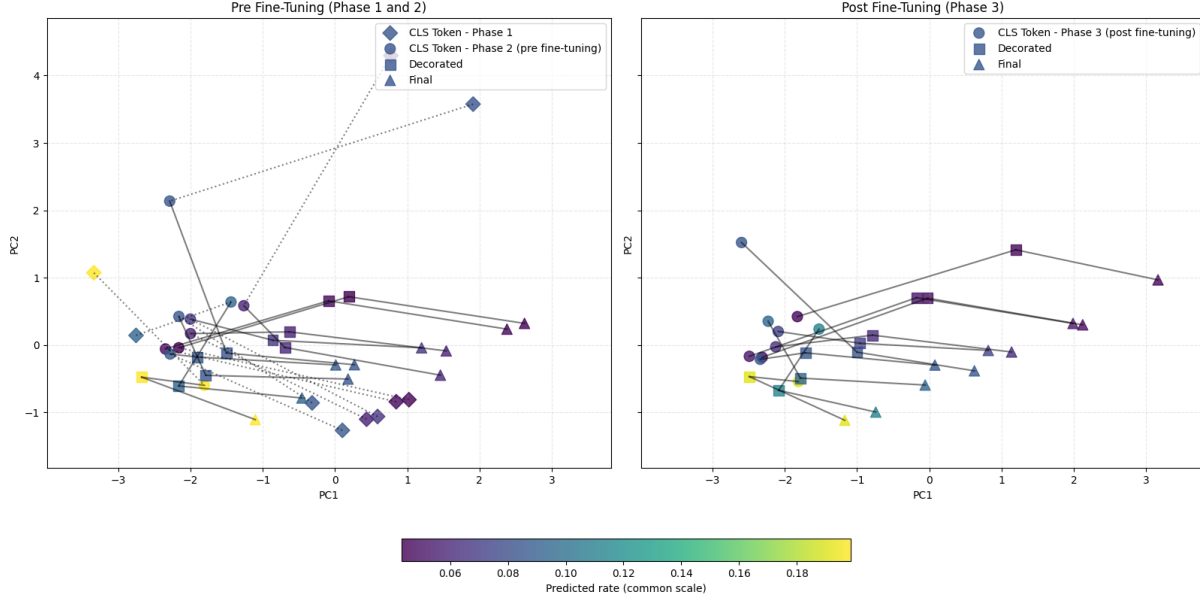


Figure 2: PCA analysis of the CLS tokens within the test set of the base Credibility Transformer model; then, we transform the following vectors from the models using this same fitted PCA analysis: the CLS token of the original CT before modifying this model, the decorated CLS tokens before ICL, the decorated CLS tokens after ICL, the CLS tokens after fine-tuning the ICL-Credibility Transformer end to end, the decorated CLS tokens after fine-tuning the ICL-Credibility Transformer and, finally, the decorated CLS tokens after fine-tuning the ICL-Credibility Transformer and performing ICL. Left panel: before full end to end fine-tuning; right panel: after full end to end fine-tuning.

B2 for points 3 and 10), after which the final stages allow plausible brand variants (B1/B3). The gains are largest in sparse slices: policies with rarer combinations – such as very young, high Bonus-Malus profiles or very old drivers paired with specific brands – seeing the greatest tightening after decoration and the most helpful, controlled broadening in the final stage (notably points 2 and 10).

5 Zero-shot analysis using ICL

5.1 Motivation for zero-shot prediction

Zero-shot prediction is used here to refer to the ability of a model to make accurate inferences on categories or feature levels that were entirely absent during model training. In practical insurance applications, this capability is crucial, as new categories may emerge over time – for example, a new vehicle model introduced by a manufacturer or an insurance product expanded to a previously uncovered geographical region. Traditional models often struggle with such unseen categories, thus, in practice, often one defaults to simple imputation of a mean or median value, or setting the categorical level to a “missing” indicator. In contrast, the ICL mechanism in the Credibility Transformer architecture enables the model to leverage contextual similarities from

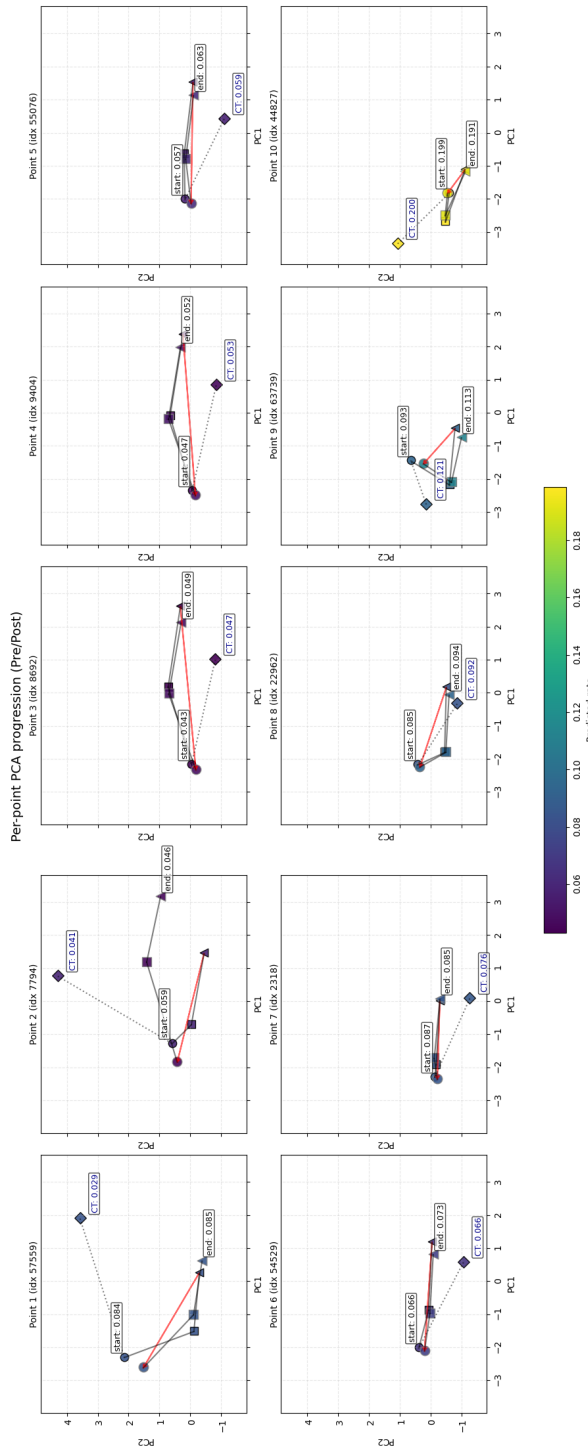


Figure 3: PCA analysis of the CLS tokens for ten points in the test set; we show the the total progression of the ten points in the PCA space, labeling the original CT predictions made for that point, the predictions after allowing the weights of the CT model to be modified and the final predictions after ICL in the fine-tuned model.

related instances, potentially generalizing to these novel cases without retraining; it is exactly this ability that we test in this section.

5.2 Set-up for zero-shot prediction

We focus on the ‘Region’ categorical feature from the French MTPL dataset and design a zero-shot experiment as follows. We create a new train-test split where certain regions are treated as completely “unseen”. Specifically, we select records comprising approximately 10% of the exposure of the entire dataset, corresponding to the regions with the lowest amounts of exposure: ['R43', 'R21', 'R42', 'R94', 'R83', 'R74', 'R23', 'R22', 'R26', 'R25', 'R73']. These regions are designated as the new test set, and their labels are remapped to a new “unseen” category to simulate novelty during inference. For the remaining training data, we further set additional region levels to “unseen” to teach the original Credibility Transformer model how to handle this category, i.e., to provide a parameter estimate for the embedding level corresponding to “unseen”. For this, we select the next smallest regions in terms of exposures – ['R41', 'R54', 'R31', 'R72', 'R91', 'R52'] – which account for roughly 20% of the exposure of the training rows. Thus, we ensure that the model encounters the “unseen” label during training, learning to rely on contextual information from similar instances. The full Credibility Transformer and ICL model pipeline are then trained on this modified dataset, and its predictive performance is assessed on the held-out test set, quantifying its zero-shot generalization to truly novel regions. Table 5.2 summarizes the key information of the train-test split. Interestingly, we see that the frequency in the new test set is a lower than in the training set; this is due to the new manner in which we have performed the split above.

Characteristic	Training set	Test set
Number of policies	601,781	76,226
Number of records set to ”unseen”	165,200	76,226
Total exposure (years)	323,458	34,900
Number of claims	24,006	2,377
Average frequency	7.42%	6.81%

Feature description
Categorical (4): Area, VehGas, VehBrand, Region
Continuous (5): VehPower, VehAge, DrivAge, BonusMalus, Density
Target: ClaimNb (claim count)
Exposure: Exposure (in years)

Table 4: Characteristics of the training and test sets for the zero-shot analysis.

5.3 Regional Analysis

As a preliminary introduction to better understand the performance of our zero-shot approach across different regions, we present a detailed breakdown of the results by region in Table 5. This table shows the claim counts, exposure, claim rates, and Poisson deviance for each region, along with whether it was designated as “unseen” and its assignment to the training or test set. The Poisson deviance has been calculated by using the average observed rates within each region as the predictions.

The regional analysis reveals interesting patterns in the distribution of risk across different geographical areas. The test regions (all designated as “unseen”) show varying claim rates ranging

Region	ClaimNb	Exposure	Claim Rate	Poisson Dev.	Unseen	Set
R43	38	564	0.07	0.215	yes	test
R21	77	1,204	0.06	0.179	yes	test
R42	92	1,209	0.08	0.273	yes	test
R94	132	1,766	0.07	0.210	yes	test
R83	141	2,322	0.06	0.187	yes	test
R74	197	2,396	0.08	0.268	yes	test
R23	220	3,177	0.07	0.178	yes	test
R22	314	3,573	0.09	0.246	yes	test
R26	345	5,023	0.07	0.219	yes	test
R25	452	6,653	0.07	0.263	yes	test
R73	369	7,014	0.05	0.158	yes	test
R41	468	8,112	0.06	0.241	yes	train
R54	800	11,163	0.07	0.271	yes	train
R31	944	11,488	0.08	0.227	yes	train
R72	1,055	14,316	0.07	0.222	yes	train
R91	1,007	14,709	0.07	0.198	yes	train
R52	1,576	21,930	0.07	0.263	yes	train
R53	1,871	27,753	0.07	0.282	no	train
R11	2,591	30,198	0.09	0.238	no	train
R93	2,986	35,749	0.08	0.240	no	train
R82	4,233	45,333	0.09	0.300	no	train
R24	6,475	102,706	0.06	0.266	no	train

Table 5: Regional breakdown showing claim counts, exposure, claim rates, and Poisson deviance by region, with designation as “unseen” and assignment to training or test sets.

from 0.05 to 0.09, with corresponding Poisson deviances between 0.158 and 0.273. Notably, regions with higher claim rates tend to have higher Poisson deviances. The training regions show a similar pattern, with the “unseen” training regions generally having lower exposure volumes than the “seen” regions also used for the initial model training. These “seen” regions have a notably higher set of claims rates and Poisson deviances than the “unseen” test set.

To provide a comprehensive view of model performance across different data segments, Table 6 presents the exposure-weighted average Poisson deviances for the key portfolio segments.

Description	Poisson Deviance
Whole portfolio	0.255
Test	0.216
Train - “unseen”	0.238
Train - region provided	0.267

Table 6: Weighted average Poisson deviances across different portfolio segments.

The weighted averages show that the test set achieves the lowest Poisson deviance (0.216), followed by the “unseen” training regions (0.238). Interestingly, the “seen” training regions with full regional information show the highest deviance (0.267).

The significant differences between train and test, and “seen” and “unseen” should be kept in

mind when understanding the zero-shot results presented in the next section, in particular, the differences between in-sample and out-of-sample results.

5.4 Zero-shot results

To evaluate the performance of the ICL-Credibility Transformer model on unseen data, the model is first trained on the training dataset. When reporting the results of all of the modeling steps, we filter the training set to assess performance only on records labeled “unseen”. Likewise, the entire test set consists of exactly these “unseen” records, but for a different set of regions, as described above. We follow the training approach outlined in Section 4: first, we fit a base Credibility Transformer model; then, we add 2 ICL layers and freeze the decoder while training for 50 epochs; finally, in the third phase, we unfreeze all weights and train for an additional 20 epochs. All other training hyper-parameters are identical to those in Table 2. The results are displayed in Table 7.

Model	# Param.	In-sample “unseen” Poisson loss	Out-of-sample Poisson loss
Null model (intercept-only)	1	23.464	21.091
base Credibility Transformer (phase 1)	15,294	22.275	20.282
ICL Transformer - 2 Layers (phase 2)	46,119	22.315	20.264
Fine-tuning ICL Transformer - 2 Layers (phase 3)	46,119	22.298	20.259

Table 7: Number of parameters, in-sample and out-of-sample Poisson deviance losses (units are in 10^{-2}). Null model has been calculated to be used as a baseline

Given that this train-test split deviates from the more conventional setup shown before, we fit a null model (intercept-only) as a baseline. The base Credibility Transformer significantly outperforms the null model on both in-sample and out-of-sample Poisson deviance losses, as we would expect. Adding ICL layers to the base Credibility Transformer (with the decoder frozen) further improves the out-of-sample loss from 20.282 to 20.264. This gain highlights the benefits of cross-record attention enriched with contextual information, as well as the role of credibility weighting, which allows tokens to enhance their predictive power by attending to other contextually similar tokens in the batch. Finally, fine-tuning the full ICL Transformer (with the decoder unfrozen) yields an additional out-of-sample improvement to 20.259. This indicates that the model benefits from adapting its decoder to the newly enriched context provided by the ICL to the CLS tokens.

Thus, we observe that the ICL-Credibility Transformer model generalizes fairly well to unseen levels, provided that it receives some training exposure to handling such unseen levels. In our example, we sacrifice information on a few low-exposure levels to allow the model to learn how to treat these missing levels. However, this approach does result in a loss of data. Alternative methods for including these levels might involve creating duplicates of records designated as “unseen” while retaining both the original and “unseen” labels. Care must be taken, however, to ensure that these training records do not serve as context for one another, as this could cause the model to perform worse on truly unseen test cases, i.e., such a leakage of information must be avoided.

6 Discussion and Conclusions

In this paper, we introduced the ICL enhanced Credibility Transformer, an architecture, which is, to our knowledge, a novel approach within the actuarial literature. This new model integrates the dynamic, example-driven learning paradigm of ICL with the robust, regularized representation learning of the Credibility Transformer. We have demonstrated empirically on the French MTPL dataset that this approach yields significant improvements in predictive accuracy, outperforming the relatively strong baseline Credibility Transformer upon which we build this new model.

A key insight of our work is the formal connection we established between the ICL mechanism and classical credibility theory. As shown in Proposition 3.1, the cross-attention layer at the heart of our ICL module functions as a sophisticated, data-driven credibility weighting scheme. The attention weights, which determine the influence of each context instance, can be interpreted as adaptive credibility factors that generalize the linear, variance-based weights of Bühlmann credibility to a non-linear, high-dimensional setting learned directly from feature interactions. Our qualitative analysis, supported by PCA and nearest-neighbor examinations, confirmed this interpretation. We observed that the ICL process refines the CLS token representations, pulling policies into more actuarially coherent clusters based on shared risk characteristics, thereby enabling more nuanced and accurate predictions.

Furthermore, the zero-shot learning experiment highlighted a particularly powerful practical advantage of the ICL-Credibility Transformer: its ability to generalize to new, unseen feature levels. By providing context from known risks that share other relevant features, the model can make better predictions for novel categories – such as a new vehicle brand or a geographical region not present in the training data – without any retraining. This capability addresses a common and persistent challenge in real-world insurance pricing, where portfolios are dynamic and new risks constantly emerge.

Looking forward beyond this initial exploration of ICL within an actuarial context, several practical issues remain. The performance of our model depends on the quality and relevance of the context batch. From a process perspective, while we employed a nearest-neighbor search in the CLS token space, scaling this retrieval process to a real world portfolios may presents a computational challenge. More importantly, a critical hurdle for practical adoption is the justification of this dynamic, context-driven approach. Regulators will demand transparency and fairness, asking why a specific set of policies was used as context for a given individual. This requires developing a way to ensure this context does not introduce biases and results in premium rates that are actuarially sound. For policyholders, the rationale must be translatable into an explanation that their rate is fine-tuned using recent, relevant, and anonymized claims experience from a peer group to ensure maximum accuracy and fairness.

References

Akyürek, E., Schuurmans, D., Andreas, J., Ma, T., and Zhou, D. (2023). What learning algorithm is in-context learning? investigations with linear models. *arXiv preprint arXiv:2211.15661*.

Brauer, A. (2024). Enhancing actuarial non-life pricing models via transformers. *European Actuarial Journal*, 14(3):991–1012.

Brown, T., Mann, B., Ryder, N., Subbiah, M., Kaplan, J. D., Dhariwal, P., Neelakantan, A., Shyam, P., Sastry, G., Askell, A., et al. (2020). Language models are few-shot learners. In *Advances in Neural Information Processing Systems*, volume 33, pages 1877–1901.

Bühlmann, H. (1967). Experience rating and credibility. *ASTIN Bulletin*, 4(3):199–207.

Bühlmann, H. and Gisler, A. (2005). *A Course in Credibility Theory and its Applications*. Springer.

Bühlmann, H. and Straub, E. (1970). Glaubwürdigkeit für Schadensätze. *Bulletin of the Swiss Association of Actuaries*, 70(1):111–133.

Devlin, J., Chang, M.-W., Lee, K., and Toutanova, K. (2019). BERT: Pre-training of deep bidirectional transformers for language understanding. In *Proceedings of the 2019 Conference of the North American Chapter of the Association for Computational Linguistics: Human Language Technologies, Volume 1 (Long and Short Papers)*, pages 4171–4186.

Dutang, C., Charpentier, A., and Gallic, E. (2024). Insurance dataset.

Garnelo, M., Schwarz, J., Rosenbaum, D., Viola, F., Rezende, D. J., Eslami, S., and Teh, Y. W. (2018). Neural processes. In *International Conference on Machine Learning*.

Gneiting, T. and Raftery, A. E. (2007). Strictly proper scoring rules, prediction, and estimation. *Journal of the American Statistical Association*, 102(477):359–378.

Gorishniy, Y., Rubachev, I., and Babenko, A. (2022). On embeddings for numerical features in tabular deep learning. *Advances in Neural Information Processing Systems*, 35:24991–25004.

Gorishniy, Y., Rubachev, I., Khrulkov, V., and Babenko, A. (2021). Revisiting deep learning models for tabular data. In *Advances in Neural Information Processing Systems*, volume 34, pages 18932–18943.

Hollmann, N., Müller, S., Eggensperger, K., and Hutter, F. (2023). TabPFN: A transformer that solves small tabular classification problems in a second. *arXiv preprint arXiv:2207.01848*.

Huang, X., Khetan, A., Cvitkovic, M., and Karnin, Z. (2020). TabTransformer: Tabular data modeling using contextual embeddings. *arXiv preprint arXiv:2012.06678*.

Johnson, J., Douze, M., and Jégou, H. (2019). Billion-scale similarity search with gpus. In *IEEE Transactions on Big Data*, volume 7, pages 535–547. IEEE.

Min, S., Lyu, X., Holtzman, A., Artetxe, M., Lewis, M., Hajishirzi, H., and Zettlemoyer, L. (2022). Rethinking the role of demonstrations: What makes in-context learning work? *arXiv preprint arXiv:2202.12837*.

Müller, S., Hollmann, N., and Hutter, F. (2024). Bayes’ power for explaining in-context learning generalizations. *arXiv preprint arXiv:2410.01565*.

Richman, R., Scognamiglio, S., and Wüthrich, M. V. (2025a). The credibility transformer. *European Actuarial Journal*. Forthcoming.

Richman, R., Scognamiglio, S., and Wüthrich, M. V. (2025b). Tree-like pairwise interaction networks. *arXiv preprint arXiv:2508.15678*.

Srivastava, N., Hinton, G., Krizhevsky, A., Sutskever, I., and Salakhutdinov, R. (2014). Dropout: a simple way to prevent neural networks from overfitting. *The Journal of Machine Learning Research*, 15(1):1929–1958.

Tancik, M., Srinivasan, P., Mildenhall, B., Fridovich-Keil, S., Raghavan, N., Singhal, U., Ramamoorthi, R., Barron, J., and Ng, R. (2020). Fourier features let networks learn high frequency functions in low dimensional domains. In *Advances in Neural Information Processing Systems*, volume 33, pages 7537–7547.

Vaswani, A., Shazeer, N., Parmar, N., Uszkoreit, J., Jones, L., Gomez, A. N., Kaiser, L., and Polosukhin, I. (2017). Attention is all you need. *Advances In Neural Information Processing Systems*, 30.

Wager, S., Wang, S., and Liang, P. S. (2013). Dropout training as adaptive regularization. *Advances in Neural Information Processing Systems*, 26.

Wei, J., Wei, J., Tay, Y., Tran, D., Webson, A., Lu, Y., Chen, X., Liu, H., Huang, D., Zhou, D., et al. (2023). Larger language models do in-context learning differently. *arXiv preprint arXiv:2303.03846*.

Wüthrich, M. V. and Merz, M. (2023). *Statistical Foundations of Actuarial Learning and its Applications*. Springer Actuarial.

Wüthrich, M. V., Richman, R., Avanzi, B., Lindholm, M., Maggi, M., Mayer, M., Schelldorfer, J., and Scognamiglio, S. (2025). AI tools for actuaries. *SSRN Manuscript*. ID 5162304.

Xie, S. M., Raghunathan, A., Liang, P., and Ma, T. (2022). An explanation of in-context learning as implicit bayesian inference. In *International Conference on Learning Representations*.

Appendix. Nearest-neighbor samples and point-level narratives

Columns shown: Stage, Rank, Distance, Exposure, Area, VehPower, VehAge, DrivAge, BonusMalus, VehBrand, VehGas, Region.

Note: We show two neighbors per stage (phase1-ct (*untrained CT*), pre-base, pre-decorated, pre-final, post-base, post-decorated, post-final).

Point 1 (selected_index 57559)

Target: Area A, VehPower 6, VehAge 18, DrivAge 68, BonusMalus 55, Brand B1, Gas Diesel, Region R53, Exposure 1.00.

Stage	Rank	Dist	Exp	Area	VP	VAge	DAge	BM	Brand	Gas	Region
phase1-ct	1	0.859284	1.00	A	6	19	69	55	B1	Diesel	R53
phase1-ct	2	0.970658	0.39	A	6	17	67	55	B1	Diesel	R53
pre-base	1	0.354658	1.00	A	6	19	69	55	B1	Diesel	R53
pre-base	2	0.358824	0.39	A	6	17	67	55	B1	Diesel	R53
pre-decorated	1	0.301852	0.39	A	6	17	67	55	B1	Diesel	R53
pre-decorated	2	0.333753	1.00	A	6	19	69	55	B1	Diesel	R53
pre-final	1	0.452421	0.39	A	6	17	67	55	B1	Diesel	R53
pre-final	2	0.680154	1.00	A	6	19	69	55	B1	Diesel	R53
post-base	1	0.471765	1.00	A	6	19	69	55	B1	Diesel	R53
post-base	2	0.474374	0.39	A	6	17	67	55	B1	Diesel	R53
post-decorated	1	0.474778	0.39	A	6	17	67	55	B1	Diesel	R53
post-decorated	2	0.528474	1.00	A	6	19	69	55	B1	Diesel	R53
post-final	1	0.544454	0.39	A	6	17	67	55	B1	Diesel	R53
post-final	2	0.874919	1.00	A	6	19	69	55	B1	Diesel	R53

Narrative. Already in phase1 (untrained) and in the pre-base model the nearest neighbors match the same A/R53 diesel B1 cohort with late-60s drivers. Outcome decoration tightens proximity (best distance $\approx 0.35 \rightarrow 0.30$) while preserving fuel/region/brand; the final stages broaden slightly but retain the same actuarial signature.

Point 2 (selected_index 7794)

Target: Area C, VehPower 4, VehAge 15, DrivAge 19, BonusMalus 90, Brand B14, Gas Regular, Region R24, Exposure 0.00 (0.0027).

Stage	Rank	Dist	Exp	Area	VP	VAge	DAge	BM	Brand	Gas	Region
phase1-ct	1	0.915045	0.43	A	4	11	24	85	B14	Regular	R24
phase1-ct	2	1.140315	0.19	A	5	13	20	90	B14	Regular	R24
pre-base	1	0.576452	0.12	C	6	17	19	90	B1	Regular	R53
pre-base	2	0.838548	0.52	B	7	16	20	85	B3	Regular	R24
pre-decorated	1	0.403106	0.12	C	6	17	19	90	B1	Regular	R53
pre-decorated	2	0.601895	0.35	C	4	11	19	85	B1	Regular	R24
pre-final	1	0.646874	0.12	C	6	17	19	90	B1	Regular	R53
pre-final	2	0.648549	0.25	A	5	16	20	90	B4	Regular	R24
post-base	1	0.956439	0.19	A	5	13	20	90	B14	Regular	R24
post-base	2	1.015568	0.52	B	7	16	20	85	B3	Regular	R24
post-decorated	1	0.787472	0.19	A	5	13	20	90	B14	Regular	R24
post-decorated	2	0.909297	0.52	B	7	16	20	85	B3	Regular	R24
post-final	1	0.918342	0.19	A	5	13	20	90	B14	Regular	R24
post-final	2	1.042231	0.52	B	7	16	20	85	B3	Regular	R24

Narrative. Phase1 already finds B14 Regulars in R24 with similar ages and high Bonus–Malus. Pre–base introduces Regular neighbors from A/C (B1/B3), and decoration tightens distances while keeping youth and Regular fuel. In the post stages, exact B14/R24 matches reappear among the closest points; final neighborhoods remain youthful, Regular and high BM.

Point 3 (selected_index 8692)

Target: Area C, VehPower 5, VehAge 1, DrivAge 60, BonusMalus 50, Brand B2, Gas Diesel, Region R24, Exposure 1.00.

Stage	Rank	Dist	Exp	Area	VP	VAge	DAge	BM	Brand	Gas	Region
phase1-ct	1	0.006281	0.17	C	5	1	60	50	B2	Diesel	R24
phase1-ct	2	0.018002	0.01	C	5	0	61	50	B2	Diesel	R24
pre-base	1	0.018674	0.01	C	5	0	61	50	B2	Diesel	R24
pre-base	2	0.037920	0.17	C	5	1	60	50	B2	Diesel	R24
pre-decorated	1	0.018339	0.01	C	5	0	61	50	B2	Diesel	R24
pre-decorated	2	0.034097	0.17	C	5	0	62	50	B2	Diesel	R24
pre-final	1	0.190356	1.00	C	5	2	64	50	B3	Diesel	R24
pre-final	2	0.201400	0.43	C	6	3	59	50	B1	Diesel	R24
post-base	1	0.016105	0.01	C	5	0	61	50	B2	Diesel	R24
post-base	2	0.033057	0.17	C	5	1	60	50	B2	Diesel	R24
post-decorated	1	0.010535	0.01	C	5	0	61	50	B2	Diesel	R24
post-decorated	2	0.034913	0.17	C	5	0	62	50	B2	Diesel	R24
post-final	1	0.196228	0.17	C	5	0	62	50	B2	Diesel	R24
post-final	2	0.204852	1.00	C	6	1	65	50	B2	Diesel	R24

Narrative. Across stages the closest neighbors are near duplicates in C/R24 with B2 diesel and ages 59–62. Decoration further tightens the best match ($\approx 0.018 \rightarrow 0.011$). Final stages admit slightly older matches (64–65, same fuel/region) but remain within the same credibility cluster.

Point 4 (selected_index 9404)

Target: Area D, VehPower 4, VehAge 0, DrivAge 57, BonusMalus 50, Brand B1, Gas Diesel, Region R24, Exposure 0.40.

Stage	Rank	Dist	Exp	Area	VP	VAge	DAge	BM	Brand	Gas	Region
phase1-ct	1	0.000000	0.84	D	4	0	57	50	B1	Diesel	R24
phase1-ct	2	0.030982	0.94	D	4	0	58	50	B1	Diesel	R24
pre-base	1	0.000000	0.84	D	4	0	57	50	B1	Diesel	R24
pre-base	2	0.071298	0.94	D	4	0	58	50	B1	Diesel	R24
pre-decorated	1	0.000000	0.84	D	4	0	57	50	B1	Diesel	R24
pre-decorated	2	0.125568	0.08	D	4	1	59	50	B1	Diesel	R24
pre-final	1	0.329011	0.49	D	4	0	60	50	B3	Diesel	R24
pre-final	2	0.360727	0.94	D	4	0	58	50	B1	Diesel	R24
post-base	1	0.000000	0.84	D	4	0	57	50	B1	Diesel	R24
post-base	2	0.065833	0.94	D	4	0	58	50	B1	Diesel	R24
post-decorated	1	0.000000	0.84	D	4	0	57	50	B1	Diesel	R24
post-decorated	2	0.116503	0.94	D	4	0	58	50	B1	Diesel	R24
post-final	1	0.195898	0.94	D	4	0	58	50	B1	Diesel	R24
post-final	2	0.308650	0.49	D	4	0	60	50	B3	Diesel	R24

Narrative. This point has near-exact duplicates (distance ≈ 0) in D/R24 B1 diesel, and decoration leaves that structure intact. Final stages admit B3/B2 variants and slightly different ages, but the local cohort remains the same.

Point 5 (selected_index 55076)

Target: Area C, VehPower 6, VehAge 5, DrivAge 50, BonusMalus 50, Brand B1, Gas Diesel, Region R52, Exposure 0.63.

Stage	Rank	Dist	Exp	Area	VP	VAge	DAge	BM	Brand	Gas	Region
phase1-ct	1	0.000000	0.36	C	6	5	50	50	B1	Diesel	R52
phase1-ct	2	0.159966	1.00	C	6	2	50	50	B1	Diesel	R52
pre-base	1	0.000000	0.36	C	6	5	50	50	B1	Diesel	R52
pre-base	2	0.052296	1.00	C	6	2	50	50	B1	Diesel	R52
pre-decorated	1	0.000000	0.36	C	6	5	50	50	B1	Diesel	R52
pre-decorated	2	0.050454	1.00	C	6	2	50	50	B1	Diesel	R52
pre-final	1	0.242212	0.49	C	7	4	47	50	B1	Diesel	R53
pre-final	2	0.263396	1.00	C	7	5	47	50	B1	Diesel	R53
post-base	1	0.000000	0.36	C	6	5	50	50	B1	Diesel	R52
post-base	2	0.057980	1.00	C	6	2	50	50	B1	Diesel	R52
post-decorated	1	0.000000	0.36	C	6	5	50	50	B1	Diesel	R52
post-decorated	2	0.054076	1.00	C	6	2	50	50	B1	Diesel	R52
post-final	1	0.207730	0.36	C	6	5	50	50	B1	Diesel	R52
post-final	2	0.231302	0.97	C	5	4	47	50	B1	Diesel	R53

Narrative. A highly redundant C/R52 B1 diesel segment: phase1 through post-decorated return a literal near-duplicate as the closest match. Final stages broaden gently into R53 with

similar ages and power.

Point 6 (selected_index 54529)

Target: Area C, VehPower 5, VehAge 2, DrivAge 46, BonusMalus 50, Brand B2, Gas Diesel, Region R72, Exposure 1.00.

Stage	Rank	Dist	Exp	Area	VP	VAge	DAge	BM	Brand	Gas	Region
phase1-ct	1	0.095599	0.45	C	5	4	46	50	B2	Diesel	R72
phase1-ct	2	0.230291	0.85	C	5	0	44	50	B2	Diesel	R72
pre-base	1	0.029398	0.45	C	5	4	46	50	B2	Diesel	R72
pre-base	2	0.149170	0.08	C	5	3	45	50	B1	Diesel	R72
pre-decorated	1	0.022880	0.45	C	5	4	46	50	B2	Diesel	R72
pre-decorated	2	0.116307	0.08	C	6	4	45	50	B2	Diesel	R72
pre-final	1	0.304717	0.59	C	5	1	42	50	B5	Diesel	R72
pre-final	2	0.330409	0.08	C	6	1	48	50	B1	Diesel	R72
post-base	1	0.030205	0.45	C	5	4	46	50	B2	Diesel	R72
post-base	2	0.143507	0.08	C	5	3	45	50	B1	Diesel	R72
post-decorated	1	0.022541	0.45	C	5	4	46	50	B2	Diesel	R72
post-decorated	2	0.122115	0.08	C	4	0	47	50	B3	Diesel	R72
post-final	1	0.226112	1.00	C	4	7	46	50	B2	Diesel	R72
post-final	2	0.271345	0.08	C	6	4	45	50	B2	Diesel	R72

Narrative. Phase1 already centres on the C/R72 B2 diesel cohort in the mid-40s. Decoration consistently tightens distances. Final stages broaden slightly to B1/B3 diesels in the same region (and occasional adjacent regions in deeper ranks), leaving the core profile unchanged.

Point 7 (selected_index 2318)

Target: Area E, VehPower 7, VehAge 2, DrivAge 61, BonusMalus 50, Brand B6, Gas Regular, Region R93, Exposure 0.21.

Stage	Rank	Dist	Exp	Area	VP	VAge	DAge	BM	Brand	Gas	Region
phase1-ct	1	0.031319	1.00	E	7	2	59	50	B6	Regular	R93
phase1-ct	2	0.124904	0.12	E	7	1	59	50	B6	Regular	R93
pre-base	1	0.043811	1.00	E	7	2	59	50	B6	Regular	R93
pre-base	2	0.050928	0.47	E	7	2	60	50	B6	Regular	R93
pre-decorated	1	0.048501	1.00	E	7	2	59	50	B6	Regular	R93
pre-decorated	2	0.056023	0.47	E	7	2	60	50	B6	Regular	R93
pre-final	1	0.221336	0.12	E	7	1	59	50	B6	Regular	R93
pre-final	2	0.317985	1.00	E	7	2	59	50	B6	Regular	R93
post-base	1	0.042100	1.00	E	7	2	59	50	B6	Regular	R93
post-base	2	0.056163	0.47	E	7	2	60	50	B6	Regular	R93
post-decorated	1	0.054033	1.00	E	7	2	59	50	B6	Regular	R93
post-decorated	2	0.071394	0.47	E	7	2	60	50	B6	Regular	R93
post-final	1	0.232991	0.47	E	7	2	60	50	B6	Regular	R93
post-final	2	0.273311	0.12	E	7	1	59	50	B6	Regular	R93

Narrative. A very stable E/R93 B6 Regular cluster: phase1 through post-decorated return practically the same neighbors (late-50s/early-60s). Final stages admit a few B6 diesel comparisons further down the list, but the area/region/fuel signature remains consistent.

Point 8 (selected_index 22962)

Target: Area E, VehPower 7, VehAge 14, DrivAge 46, BonusMalus 54, Brand B2, Gas Regular, Region R82, Exposure 1.00.

Stage	Rank	Dist	Exp	Area	VP	VAge	DAge	BM	Brand	Gas	Region
phase1-ct	1	0.569729	1.00	E	7	13	43	54	B1	Regular	R82
phase1-ct	2	0.734658	1.00	E	5	11	45	54	B3	Regular	R82
pre-base	1	0.416628	1.00	E	7	13	43	54	B1	Regular	R82
pre-base	2	0.561383	0.18	E	7	12	42	54	B1	Regular	R82
pre-decorated	1	0.359361	1.00	E	7	13	43	54	B1	Regular	R82
pre-decorated	2	0.455073	0.18	E	7	12	42	54	B1	Regular	R82
pre-final	1	0.412044	1.00	E	7	13	43	54	B1	Regular	R82
pre-final	2	0.478571	0.18	E	7	12	42	54	B1	Regular	R82
post-base	1	0.481606	1.00	E	7	13	43	54	B1	Regular	R82
post-base	2	0.521648	0.16	E	6	13	43	55	B5	Regular	R82
post-decorated	1	0.348787	1.00	E	7	13	43	54	B1	Regular	R82
post-decorated	2	0.409371	0.16	E	6	13	43	55	B5	Regular	R82
post-final	1	0.350916	1.00	E	7	13	43	54	B1	Regular	R82
post-final	2	0.517703	0.18	E	7	12	42	54	B1	Regular	R82

Narrative. A clear E/R82 Regular cohort with ages in the low- to mid-40s. Decoration reliably tightens the closest match. Post stages occasionally draw B5 Regulars (or B1 diesels farther down), but region and age alignment remain strong.

Point 9 (selected_index 63739)

Target: Area E, VehPower 8, VehAge 13, DrivAge 35, BonusMalus 72, Brand B1, Gas Regular, Region R11, Exposure 0.18.

Stage	Rank	Dist	Exp	Area	VP	VAge	DAge	BM	Brand	Gas	Region
phase1-ct	1	0.349907	1.00	E	8	12	34	72	B1	Regular	R11
phase1-ct	2	0.487421	0.85	E	6	11	34	76	B1	Regular	R11
pre-base	1	0.323057	1.00	E	8	12	34	72	B1	Regular	R11
pre-base	2	0.585882	0.91	E	8	11	33	72	B1	Regular	R11
pre-decorated	1	0.250448	1.00	E	8	12	34	72	B1	Regular	R11
pre-decorated	2	0.378647	0.25	C	5	4	31	80	B6	Regular	R31
pre-final	1	0.471002	0.08	C	7	14	32	81	B6	Diesel	R72
pre-final	2	0.492369	0.08	E	5	9	28	76	B5	Regular	R26
post-base	1	0.284585	1.00	E	8	12	34	72	B1	Regular	R11
post-base	2	0.514235	0.91	E	8	11	33	72	B1	Regular	R11
post-decorated	1	0.209932	1.00	E	8	12	34	72	B1	Regular	R11
post-decorated	2	0.383713	0.91	E	8	11	33	72	B1	Regular	R11
post-final	1	0.363904	1.00	E	8	12	34	72	B1	Regular	R11
post-final	2	0.487113	0.08	E	7	8	33	72	B1	Regular	R11

Narrative. The dominant pattern is E/R11 Regular B1 with early- to mid-30s drivers. Decoration tightens substantially (best distance $\approx 0.32 \rightarrow 0.21$ pre; $\approx 0.28 \rightarrow 0.21$ post). Pre-final briefly explores B6 diesel (R72) and B5 Regular (R26), but post stages re-centre on R11 Regular B1.

Point 10 (selected_index 44827)

Target: Area C, VehPower 4, VehAge 4, DrivAge 21, BonusMalus 95, Brand B2, Gas Diesel, Region R24, Exposure 0.15.

Stage	Rank	Dist	Exp	Area	VP	VAge	DAge	BM	Brand	Gas	Region
phase1-ct	1	0.528064	0.24	C	5	2	24	95	B2	Diesel	R24
phase1-ct	2	0.584082	0.16	C	5	3	21	95	B2	Diesel	R24
pre-base	1	0.159332	0.16	C	5	3	21	95	B2	Diesel	R24
pre-base	2	0.322642	0.01	C	5	1	19	95	B2	Diesel	R24
pre-decorated	1	0.226593	0.16	C	5	3	21	95	B2	Diesel	R24
pre-decorated	2	0.376376	0.36	C	5	6	20	95	B3	Diesel	R53
pre-final	1	0.553746	0.44	A	6	5	24	95	B2	Diesel	R24
pre-final	2	0.575868	0.66	D	7	10	23	95	B6	Regular	R24
post-base	1	0.219119	0.16	C	5	3	21	95	B2	Diesel	R24
post-base	2	0.402813	0.13	C	6	9	21	95	B1	Diesel	R24
post-decorated	1	0.265050	0.16	C	5	3	21	95	B2	Diesel	R24
post-decorated	2	0.326072	0.44	A	6	5	24	95	B2	Diesel	R24
post-final	1	0.510366	0.01	C	5	1	19	95	B2	Diesel	R24
post-final	2	0.623841	0.16	C	5	3	21	95	B2	Diesel	R24

Narrative. A young, high-BM B2 diesel in C/R24 has strong near duplicates from phase1 onwards. Decoration modestly broadens the local set (occasional B3 diesel and A/R24). Final stages keep B2 diesel neighbors in R24 with small shifts in age and power, preserving the core risk profile.